Computational modelling of cellular effects post-irradiation with low- and high-LET particles and different absorbed doses

Adriana Alexandre S. Tavares and João Manuel R. S. Tavares

Faculdade de Engenharia, Universidade do Porto

Rua Dr. Roberto Frias, S/N, 4200-465, Porto, Portugal

Email addresses: adriana_tavares@msn.com; tavares@fe.up.pt

Running title: Computational modelling of cellular effects post-irradiation

Corresponding Author:

Prof. João Manuel R. S. Tavares

Faculdade de Engenharia, Universidade do Porto

Departamento de Engenharia Mecânica

Rua Dr. Roberto Frias, s/n, 4200-465 PORTO, PORTUGAL

Phone: +315 22 5081487, Fax: +315 22 5081445

Email: tavares@fe.up.pt Url: www.fe.up.pt/~tavares

Abstract

The use of computational methods to improve the understanding of biological responses to various types of radiation is an approach, where multiple parameters can be modelled and a variety of data is generated. This study compares cellular effects modelled for low absorbed doses against high absorbed doses. The authors hypothesized that low and high absorbed doses would contribute to cell killing via different mechanisms, potentially impacting on targeted tumour radiotherapy outcomes. Cellular kinetics following irradiation with selective low- and high-linear energy transfer (LET) particles were investigated using the Virtual Cell (VC) radiobiology algorithm. Two different cell types were assessed using the VC radiobiology algorithm: human fibroblasts and human crypt cells. The results showed that at lower doses (0.01 to 0.2 Gy), all radiation sources used were equally able to induce cell death ($p>0.05$, ANOVA). On the other hand, at higher doses (1.0 to 8.0 Gy), the radiation response was LET and dose dependent ($p<0.05$, ANOVA). The data obtained suggests that the computational methods used might provide some insight into the cellular effects following irradiation. The results also suggest that it may be necessary to re-evaluate cellular radiation-induced effects, particularly at low doses that could affect therapeutic effectiveness.

Key words: computational methods, radiation-induced effects, cell kinetics, bystander effect, targeted tumour radiotherapy, Auger electrons, alpha particles, beta particles

1. Introduction

The Virtual Cell (VC) radiobiology simulator, was developed by Stewart and co-workers (Stewart 2004), to evaluate the following cellular endpoints: cell death, neoplastic transformation, chromosome aberration yields, induction of genomic instability, cell cycle kinetics and the probability of tumour eradication following radiation therapy. This simulator relies on multiscale modelling, which is essentially an integrative approach of multiple "sub-models" that are tested against measured data from *in vitro* systems. Thus, in order to model the emergent response of a group of cells or a tissue, these sub-models are linked together to form a "supermodel". The postulated mechanisms, resulting from the multiscale supermodel, are subsequently compared to data from *in vivo* systems. This algorithm is an ongoing effort that aims to understand tumour pathogenesis and treatment; however, due to the complexity associated with such phenomena, simplified radiobiological models were used (Stewart 2004). Modelling cellular environments and cellular responses to irradiation by computational methods is complex and challenging. Radiation-induced effects are not yet fully understood, and regularly, new knowledge is added.

An important contribution from recent research to the field of cellular radiobiology was the evidence supporting the existence of radiation-induced bystander effects, i.e. effects detected in cells that were not directly "hit" by an ionizing radiation track (Boyd *et al.* 2006; Brooks 2004; Kassis 2003; Mothersill *et al.* 2003; Nagasawa *et al.* 2003; Persaud *et al.* 2005; Snyder 2004; Sokolov *et al.* 2005). Results from studies investigating radiation-induced bystander effects suggest that this effect will have implications on targeted radiotherapy microdosimetric estimates (Boswell *et al.* 2005; Britz-Cunningham *et al.* 2003; Kassis 2003) and on the current central radiobiological paradigm, where all radiation events are contained in the "hit" cell (Mothersill *et al.* 2003; Nagasawa *et al.* 2003). Multiple studies have found that radiation causes "hit" cells to produce signals that can be received by cells close or distant from the targeted cell, named recipient cells. In turn, these recipient cells transduce signals and coordinate a response, named adaptive response. Such coordinated response can be protective, for example, when an apoptotic response is initiated to remove abnormal cells from the population (Mothersill *et al.*

2006). These responses do not seem to be dependent on the absorbed dose nor the radiation quality but appear to be dependent on genetic and environmental influences (Lyng *et al.* 2002; Mothersill *et al.* 2006; Snyder 2004; Sokolov *et al.* 2005). The multiple observations demonstrating that the bystander effects and the adaptive response are independent of radiation quality further reinforce the use of less conventional particles for targeted tumour radiotherapy, such as Auger electrons (Boswell *et al.* 2005; Boyd *et al.* 2006; Britz-Cunningham *et al.* 2003; Sofou 2008; Tavares *et al.* 2010a).

The cellular endpoints associated with the bystander effects include: mutation, gene induction, micronuclei formation, cell transformation and cell killing (Lyng *et al.* 2002; Mothersill *et al.* 2003; Nagasawa *et al.* 2003). These endpoints show a similar dose dependency, and therefore may be closely associated. In addition, bystander effects and genomic instability are both induced at very low doses, and there is evidence that bystander signals can induce genomic instability both *in vitro* and *in vivo* (Koturbash *et al.* 2006; Lyng *et al.* 2002; Mothersill *et al.* 2003). The authors hypothesized that the use of a VC radiology simulator could be used to evaluate different cellular endpoints, including cell death and the induction of genetic instability, in order to investigate different aspects of cellular responses following irradiation. This paper aims to model cellular responses following irradiation with a wide range of absorbed doses and linear energy transfer (LET), in order to better understand the mechanisms that contribute to cell killing at low and high absorbed doses. Cell irradiation using Auger electrons, alpha particles and beta minus particles were modelled using the VC simulator and different irradiation scenarios.

2. Methods

Previous studies have shown that the Technetium-99m (^{99m}Tc) CKMMX electron (all M-shell Coster–Kroning (CK) and super-CK transitions, E = 1.16×10^{-4} MeV) and Auger MXY (all M-shell Auger transitions, E = 2.26×10^{-4} MeV) could be classified as high LET particles, similar to Astatine-211 (^{211}At, E = 6.79 MeV) alpha particles and in contrast to the Iodine-131 (^{131}I, E = 0.606 MeV) beta minus particles, which are low LET particles (Tavares *et al.* 2010b).

Therefore, in this study the ^{99m}Tc CKMMX electrons and Auger MXY were used as high LET Auger emitters, the ^{211}At alpha particles as high LET alpha emitters and the ^{131}I beta minus particles as low LET emitters. The Monte Carlo damage simulation (MCDS) algorithm was used to obtain the number of double strand breaks (DSB) and the percentage of complex DSB (FCB) (Semenenko *et al.* 2005; Stewart 2004) for each investigated particle as previously reported (Tavares *et al.* 2010b). The MCDS simulator is a fast Monte Carlo algorithm that models the damages to DNA by different radioactive particles and captures the major trends in the DNA damage spectrum predicted using detailed track structure simulations (Semenenko *et al.* 2004). The results obtained from the MCDS simulator (DSB and FCB) that express the damage caused by the radioactive particle to the DNA per Gy per cell, were then applied as input parameters for the two-lesion kinetics (TLK) model used on the VC simulator. The TLK model was preferred over other radiation exposure models, such as the repair-misrepair model (RMR) and lethal-potentially lethal model (LPL), as it applies an improved correlation between the biochemical processes of DSB and cell death, by subdividing DSB into simple or complex DSBs (Guerrero *et al.* 2002; Sachs *et al.* 1997; Stewart 2004; Tavares *et al.* 2010b). A comprehensive list with all input parameters used on the VC simulations is presented in next section.

2.1 VC Simulator – Input Parameters

In this section only key VC input parameters used for the present study will be discussed, since an online platform, including a comprehensive VC user guide, is freely available on-line (http://faculty.washington.edu/trawets/vc/ug/index.html).

The cell kinetics model (CKM) used was the quasi-exponential cell kinetics model (QECK), as that is the only available option for the current version of the VC simulator. Nonetheless, by using a high peak cell density (KAP) value (such as the one used in the present study, i.e. 1.0E+38 cells/cm^3, Table 1) and by selecting a small initial cell population (initial number of cells – N0 = 1000 cells) compared to KAP×VOL (where VOL = tissue volume = 1 cm^3, Table 1), the cell growth kinetics model becomes exponential. Furthermore, as the size of

the cell population approaches KAP×VOL, the net cell birth rate decreases so that the cell population size approaches the asymptotic value KAP×VOL. The cell's DNA content at the G0 or G1 phase on the cell cycle and the number of chromosomes per cell (Table 1) were selected based on currently available biological knowledge of the human cell and human genome. Two different cell types were evaluated: 1) human fibroblasts (TPOT - cell doubling time=0.667 days = 16 hours) and 2) human intestinal crypt cells (TPOT=1.625 days = 39 hours) (Baserga 1971; Baserga 1993; Tavares *et al.* 2010b). The evaluated populations were set to be heterogeneous, with cycling and quiescent cells (GF – growth fraction=0.5), in order to mimic as close as possible the cellular biological reality *in vitro*, where dividing and quiescent cells coexist. The expected number of DSBs endogenously formed per cell-hour was set at 4.3349E-03 Gy^{-1} $cell^{-1}$(Table 1). This value was chosen based on a study conducted by Stewart in 1999 (Stewart 1999).

The values of the biophysical parameters: repair half-time (RHT), pairwise damage interaction rate (ETA) and probability of correct repair (A0) were set according to the requisites of the selected damage repair model. For example, the TLK model used sets the RHT, ETA and A0 values at certain intervals, including those described in Table 1. The probability of misrejoined DSB being lethal (PHI) and the fraction of residual damage at the end of the simulation that is treated as lethal (FRDL) are adjustable parameters. The absolute residual damage cutoff (ACUT) value is also an adjustable parameter, and it terminates the simulation when the amount of unrepaired residual damage is less than the specified value. It is reasonable to accept that after a certain level of residual damages, any further cellular killing can be neglected as non-radiation related. The ACUT value of 1.0×10^{-09} expected number of DNA damages per cell was chosen based on the fact that it should be smaller than the spontaneous endogenous damages (established to be in the order of 10^{-3}) and a value of zero would not terminate the simulation, since ACUT was the only simulation control parameter adopted in the present study. An ACUT value of 1.0×10^{-09} would correspond to approximately 10 days after irradiation. The fraction of binary-misrepaired damages that are lethal (GAM) was set at 0.25 (Table 1), because according to Sach and co-workers, 1997, around 1/4 of the chromosome

aberrations formed through the pairwise interaction process are lethal (i.e., GAM=0.25) (Sachs *et al.* 1997).

The radiation exposure scenario selected was the exponentially decreasing dose rate (DECAY), since the present work aimed at modelling the cellular responses to different absorbed doses in a scenario of internal targeted radiotherapy using 3 radioisotopes (^{99m}Tc, ^{211}At and ^{131}I). For each radioisotope investigated, a radioactive constant (LAM) and a radionuclide half-life (RHL) was set according to the well known decay scheme of these radioisotopes. The average background absorbed dose rate on planet Earth (BGDR) has been quantified as 2.73748×10^{-7} Gy/h by the United Nations Scientific Committee on the Effects of Atomic Radiation (UNSCEAR) 2007 report (UNSCEAR 2007). Irradiation periods of 2 hours (TCUT, i.e. time cutoff parameter set at 2 hours) with total absorbed doses delivered to the cell system over all time (TAD) ranging between 0.01 and 8 Gy were modelled using the VC simulator. The effective dose delivered to the cell system in a finite time interval (0, TCUT), i.e. the SAD parameter is related to the TAD parameter by: SAD = (1-DCUT)×TAD, where DCUT = the dose cutoff used to truncate dose rate function after fraction 1-DCUT of total dose has been delivered. The DCUT is an adjustable parameter of the VC simulator and in this study was set at 0.01, which means that the dose rate is truncated only after 99% of the set effective dose (SAD) has been delivered. This meant that SAD ≈ TAD. The use of the DCUT parameter is justifiable since at a given point, the radioactivity of the radiation source becomes so small that any further radiation killing of the cell population can be neglected. The time to execute a DECAY simulation tends to increase as the number of steps increases. It is possible to control that by using the step-size tolerance (STOL) parameter, that typically ranges from about 0.05 to 1.0×10^{-3} Gy/h. As the STOL value decreases, the time requested to perform the simulation increases and thus, a compromise between time and accuracy must be made. In the present study, a STOL value of 0.01 Gy/h was used (Table 1).

A detailed description of the algorithm parameters used in the VC input file is given in Table 1.

2.2 Data analysis

The VC data was expressed as the number of direct lethal damages per surviving cell, estimated number of surviving cells, probability of mutagenesis and enhanced genetic instability per surviving cell, neoplastic transformation frequency per irradiated cell and neoplastic transformation frequency per surviving cell. In addition to analysis of the results, including data from the whole range of the investigated absorbed doses, the results were also grouped as lower and higher absorbed doses. Since this paper is investigating the differences between cellular response to low and high absorbed doses, in the context of radiotherapy using radioactive particles, the cutoff value was 1.0 Gy. The lower doses were defined as those < 1.0 Gy, while higher doses were defined as doses ≥ 1.0 Gy. This criterion was based on previous findings showing that the cellular response to doses below 0.5 Gy would have a significant contribution from the bystander effect, while cellular response to doses above 0.5 Gy would behave as dose-dependent (Seymour *et al.* 2000). Data differences from among the investigated radioisotopes for the same absorbing doses were analysed using the ANOVA statistical test, where $p<0.05$ was considered statically significant.

3. Results

The estimated number of fibroblasts and crypt cells that survived irradiation when the cell population was heterogeneous (with quiescent cells and actively cycling cells) is presented in Figures 1(a) and 1(b), respectively. The results showed that the cell survival peaks at different doses, depending on the radioactive particle (^{99m}Tc electrons and ^{211}At alpha particles peak at around 0.15 and 0.2 Gy, while ^{131}I peaks at around 1.5 and 2.0 Gy). Statistical analysis revealed no differences among the radioactive particles, when the whole irradiation range was considered ($p=0.77$, ANOVA). When dividing the evaluated dose range into lower irradiation doses (< 1.0 Gy) and higher irradiation doses (≥ 1.0 Gy), no statically significant differences were observable between distinct radioactive particles for lower doses ($p=0.08$ for fibroblasts and $p=0.19$ for crypt cells, ANOVA). However, statistically significant differences were seen for higher irradiation doses ($p=0.03$ for fibroblasts and $p=0.02$ for crypt cells, ANOVA).

Figure 2 shows the mutagenesis and enhanced genetic instability probability per surviving cell for different irradiating sources. Analysis of these curves reveals that the probability of mutagenesis and enhanced genetic instability of the cell population following irradiation with ^{99m}Tc selected electrons and ^{211}At alpha particles (high-LET particles) increased from 0 to 1.0 Gy, peaking at those absorbed dose levels and returning to negligible values at approximately 4.0 Gy. Conversely, a curve peak shifting was observed for ^{131}I beta minus particles (low-LET particles) in comparison to the other irradiation sources. The highest probability of mutagenesis and enhanced genetic instability of the cell population following irradiation with ^{131}I beta minus particles was found at 4.0 Gy and negligible levels of mutagenesis and enhanced genetic instability post-peak were not reached even at doses as high as 8.0 Gy. Statistical analysis of the whole dose range reveals no differences between the investigated radioactive particles ($p=0.49$, ANOVA). However, when the duality lower dose/higher dose was taking into account (lower doses of <1.0 Gy; and higher doses of $\geq$ 1.0 Gy), statistically significant differences were found in each tail of the curves ($p=0.00$ for low doses and $p=0.04$ for high doses).

The neoplastic transformation frequency per irradiated cell and per surviving cell for each evaluated particle is shown in Figure 3a and 3b, respectively. The probability of neoplastic transformation per irradiated cell was highest for lower doses, regardless of the radioactive particle used, and reduced as the dose increased (Figure 3a). Conversely, the probability of neoplastic transformation frequency per surviving cell was lowest for low absorbed doses and increased as the absorbed dose increased (Figure 3b). The reduction rates of neoplastic transformation frequency per irradiated cell varied for low- and high-LET particles, where the steepest reduction was observed for high-LET particles, and a slower reduction was found for low-LET particles. Statistically significant differences were observed among distinct radioactive particle neoplastic transformation frequencies per irradiated cell ($p=0.00$, ANOVA). In a similar manner, the increase rate of neoplastic transformation frequency per surviving cell varied for low- and high-LET particles, where the steepest increase was observed for high-LET particles, and a slower increase was determined for low-LET particles ($p=0.00$, ANOVA).

Finally, Figure 4 shows the number of direct lethal damages per surviving cell as a function of absorbed dose. The results showed a rapid increase in cellular lethal damages as the absorbed dose increased, where statistically significant differences were observed among distinct radioactive particles (p=0.00, ANOVA).

4. Discussion

The results showed that the estimated number of surviving cells increased, peaked and decreased as a function of absorbed dose, describing a non-linear parabolic-type curve (Figure 1). No differences were found among distinct radioactive particles for lower absorbed doses, but differences were observed at higher absorbed doses. The absence of differences among distinct radioactive particles for lower doses, suggests that another factor, other than radiation quality, may be responsible for the inexistence of differences among the radioactive particles. Conversely, at higher doses, the cell response appears to behave in a LET and dose dependent manner. To further clarify the nature of the non-linear curve following irradiation of human fibroblasts and human crypt cells with different radioactive particles, three cellular endpoints were assessed by computational simulation: mutagenesis and enhanced genetic instability per surviving cell (Figure 2), neoplastic transformation per irradiated or surviving cell (Figure 3) and number of direct lethal damages per surviving cell (Figure 4).

Mutagenesis and enhanced genetic instability results showed that there is a non-linear relationship between genomic instability and absorbed dose (Figure 2), which is in agreement with previous observations (Mothersill *et al.* 2003; Seymour *et al.* 2000). Sokolov and co-workers in 2005, using primary human fibroblasts, found that for doses of alpha particles and gamma rays between 0.2 and 0.6 Gy, the number of DSB sites in bystander cells was higher than for doses of 2.0 Gy (Sokolov *et al.* 2005). DNA DSBs have been associated with genetic instability, which is one of the mechanisms underlying the bystander effect. The results from the VC simulator showed that the probability of mutagenesis and genetic instability for alpha particles (and the other high LET particles investigated) was higher for doses ranging between 0.2 and 1.5 Gy than for doses equal to or above 2.0 Gy (Figure 2). These findings seem to be in

line with *in vitro* observations reported by Sokolov and co-workers in 2005 (Sokolov *et al.* 2005).

The data also showed that probability of cell transformation per irradiated cell was higher for lower absorbed doses (Figure 3a), while the probability of cell transformation per surviving cell (Figure 3b) and the number of direct lethal damages per surviving cell (Figure 4) was higher for high absorbed doses. Redpath and co-workers studies have also reported that the cell transformation frequency per surviving cell increased with increasing absorbed doses (Pant *et al.* 2003; Redpath 2006; Redpath *et al.* 2007). Other studies have found that as the absorbed dose increased, the direct damage component of cellular response to radiation increased, and at doses around 0.1-0.4 Gy the direct damage component was the main contributor responsible for the cellular response to irradiation (Brenner *et al.* 2001; Leonard 2008). Results from the VC simulator are in line with these observations.

Taken all together, these data show that, at the lower absorbed doses, the genetic instability of surviving cells and the transformation frequency per irradiated cell are the two major contributors for the low number of estimated surviving cells, since the values of direct lethal damages and transformation frequency per surviving cell for lower doses are small compared with higher absorbed doses. Conversely, at higher absorbed doses, cell death is mainly related to the number of direct lethal damages, the transformation frequency per surviving cell and the radiation quality. This does not mean that genetic instability of surviving cells and transformation frequency per irradiated cell effects have no relevance at higher doses but that their relative importance as a portion of the total effect tends to decrease as the dose increases. Previous studies have pointed out similar conclusions (Mothersill *et al.* 2003; Seymour *et al.* 2000) providing confidence in this model and the results obtained here. Another study by Liu and co-workers in 2007, using computational models and HPV-G human skin keratinocytes exposed to gamma rays, found that for doses above 0.3 to 0.5 Gy, the survival response of the bystander cells reached a plateau, suggesting that the emission of bystander signals may be saturated at that point (Liu *et al.* 2007). This would mean that for doses above 0.3 to 0.5 Gy, the cellular response to radiation will be mainly dependent on direct radiation

effects rather than on bystander effects, such as, genetic instability and irradiated cell transformation (Koturbash *et al.* 2006; Lyng *et al.* 2002; Mothersill *et al.* 2003). The experimental scenarios modelled by Liu and co-workers, that were validated using *in vitro* medium transfer experiments (Liu *et al.* 2007), agree with the results using the VC simulator, which further provide confidence in the simulator used in this paper. An interpretation of the low number of surviving cells obtained for lower absorbed doses could be the protective adaptive response, where the genetic instability in surviving cells and the neoplastic transformation of irradiated cells would result in a triggering of the apoptotic response to eliminate damaged cells from the population. This type of adaptive response can be classified as a positive outcome of the bystander effects (Leonard 2008; Mothersill *et al.* 2006).

Given the close links found between genetic instability, cell transformation and the bystander effect (Koturbash *et al.* 2006; Lyng *et al.* 2002; Mothersill *et al.* 2003), the VC simulator might be useful as a first line screening tool for prediction and modelling of cellular effects and possibly the bystander effects at lower absorbed doses. Although this cannot be taken as granted without *in vitro* studies performed under the same conditions as those modelled in the VC simulator. The data obtained from the VC simulator should be interpreted with caution due to the parameter estimation issues associated with mechanism-based radiation response models. Although flexibility in changing input parameters will have obvious advantages by allowing the modelling of multiple irradiation scenarios, it also represents an issue due to the uncertainty associated with the choice of a certain value in detriment of another. Together with *in vitro* or *in vivo* studies data, the simulators such as the one presented in this work, would allow better experimental design and could be used to study different processes associated with cell response to ionizing radiation. Thus, future *in vitro* and *in vivo* studies are crucial to establish a definite role of the simulator used here and careful interpretation of the results is therefore recommended. Another important consideration regarding the use of models for studying cellular effects of low doses of radiation is the fact that radiobiology models do not accommodate new findings. This means that future research may deem the VC simulator useful or obsolete. In addition, as long as the mechanisms of radiation induced cellular effects for low

absorbed doses remain unclear, modelling low dose effects is difficult and uncertainty is high. In fact, the identification of models to better quantify the cellular response to low doses of radiation is one of the key challenges facing the radiation research community (Stewart *et al.* 2006). Nevertheless, the comparative analysis of the VC generated data with prior studies (discussed above), support the use of the VC simulator as a useful tool in the field of radiobiology, with particular interest in the context of radiotherapy. Several other mathematical models have been proposed to quantify the impact of low absorbed doses on the dose-response curves for ionizing radiation (Brenner *et al.* 2001; Fornalski *et al.* 2011; Leonard 2008; Little *et al.* 2005; Nikjoo *et al.* 2003).

In this paper, the use of computational methods to model an internal radiotherapy scenario, where the radioisotope is inserted close to the cell nucleus, was investigated. This is of key importance in targeted tumour radiotherapy, because if the radioisotope was decaying outside the cell or in the cell cytoplasm, the outcome would be different, as shown in previous studies investigating the relationship between the decay site distance to the cell nucleus and the energy deposition into the DNA molecule (Boyd *et al.* 2006; Humm *et al.* 1994; Tavares *et al.* 2010a). Under the modelled scenario here, the work contributes to the current literature on targeted radiotherapy by pin-pointing that cellular effects at low doses can be an important contribution for microdosimetric estimations and may impact the therapeutic effectiveness prediction. Furthermore, the findings further support the current view that the overall “target” population after irradiation exposure at lower doses might be larger than that predicted using the traditional dosimetric methods. The results using the VC simulator suggest that targeted tumour radiotherapy with low absorbed doses might be as efficient in cell killing as very high absorbed doses, despite the cell mechanisms associated with each side of the dose-response curve (low *versus* high absorbed doses) being considerably different. This study focused on targeted tumour radiotherapy scenarios, where the radioactive source was inserted near the cell nucleus. The radioisotopes studied included beta emitters, Auger electrons emitters and alpha emitters, covering the most commonly used particles in current targeted tumour radiotherapy. Doses ranging 1 cGy and 8.0 Gy were tested on heterogeneous cell populations and the number of

surviving cells following irradiation was estimated. Nonetheless, if the purpose was to investigate cellular response in the context of domestic or occupational exposure to ionizing radiation, i.e. radiation protection studies, the exposure scenarios would have to be modelled in a different manner. Both targeted tumour radiotherapy studies and radiation protection studies can be modelled using the VC simulator by altering the input conditions, such as the number of DSB and fraction of complex DSB, the damage-repair model or other parameters. The VC simulator is a user friendly platform that provides output data consistent with experimental terminology used by cellular radiobiologists. This might foster the future use of the VC simulator by non-computer scientists, by using a similar approach as the one described here.

In conclusion, data obtained using the VC simulator indicate that low doses of all tested radioactive particles (^{99m}Tc Auger electrons, ^{211}At alpha particles and ^{131}I beta minus particles) seem to be equally able to induce cell death independently of their LET. At low doses cell death was found to be due to high genetic instability and cell transformation that are cellular endpoints measured when investigating the bystander effect. On the contrary, at high absorbed doses, cellular response to radiation seems to be dose and LET dependent. These findings can impact targeted tumour radiotherapy outcome predictions and suggest that the traditional radiobiological paradigm of radiation-induced effects contained in the “hit” cell may be obsolete. In addition, the data here suggest that the use of novel therapeutic approaches with unconventional types of radioisotopes may hold promise for targeted tumour radiotherapy.

Acknowledgements

The authors wish to thank Dr Robert Stewart (School of Health Sciences – Purdue University, USA) for providing the simulator software package used and for his kind technical assistance.

References

Baserga R. 1971. The Cell Cycle and Cancer. In: Farber E (ed), The Biochemistry of Disease - A Molecular Approach to Cell Pathology - Volume I, pp. 22. Marcel Dekker, USA

Baserga R. 1993. Definig the Cycle. In: Sadava D (ed), Cell Biology - Organelle Structure and Function, pp. Jone and Barlett Publishers, USA

Boswell C and Brechbiel M. 2005. Auger Electrons: Lethal, Low Energy, and Coming Soon to a Tumor Cell Nucleus Near You. J Nucl Med 46:1946-1947

Boyd M, Ross S, Dorrens J, Fullerton N, Tan K, Zalutsky M and Mairs R. 2006. Radiation-Induced Biologic Bystander Effect Elicited In Vitro by Targeted Radiopharmaceuticals Labeled with a, b and Auger Electrons Emitting Radionuclides. J Nucl Med 47:1007-1015

Brenner D, Little J and Sachs R. 2001. The Bystander Effect in Radiation Oncogenesis: II. A Quantitative Model. Radiat Res 155:402-408

Britz-Cunningham S and Adelstein J. 2003. Molecular Targeting with Radionuclides: State of the Science. J Nucl Med 44:1945-1961

Brooks AL. 2004. Evidence for "bystander effects" *in vivo*. Hum Exp Toxicol 23:67-70

Fornalski KW, Dobrzynski L and Janiak MK. 2011. A Stochastic Markov Model of Cellular Response to Radiation. Dose-Response 9:477- 496

Guerrero M, Stewart R, Wang J and Li X. 2002. Equivalence of linear-quadratric and two-lesion kinetic models. Phys Med Biol 47:3197-3209

Humm J, Howell R and Rao D. 1994. Dosimetry of Auger-Electron-Emitting Radionuclides. Med Phys 21:1901-1915

Kassis A. 2003. Cancer Therapy with Auger Electrons: Are We Almost There? J Nucl Med 44:1479-1481

Koturbash I, Rugo RE, Hendricks CA, Loree J, Thibault B, Kutanzi K, Pogribny I, Yanch JC, Engelward BP and Kovalchuk O. 2006. Irradiation induced DNA damage and modulates epigenetic effectors in distant bystander tissue *in vivo*. Oncogene 25:4267-4275

Leonard B. 2008. A Review: Development of a Microdose Model for Analysis of Adaptive Response and Bystander Dose Response Behavior Dose-Response 6:113-183

Little M, Filipe J, Prise KM, Folkard M and Belyakov O. 2005. A model for radiation-induced bystander effects, with allowance for spatial position and the effects of cell turnover. J Theor Biol 232:329-338

Liu Z, Prestwich W, Stewart R, Byun S, Mothersill C, McNeill F and Seymour C. 2007. Effective Target Size for the Induction of Bystander Effects in Medium Transfer Experiments. Radiat Res 168:627-630

Lyng FM, Seymour C and Mothersill C. 2002. Early Events in the Apoptotic Cascade Initiated in Cells Treated with Medium from the Progeny of Irradiated Cells. Radiat Prot Dosimetry 99:169-172

Mothersill C and Seymour C. 2003. Radiation-induced bystander effects, carcinogenesis and models. Oncogene 22:7028-7033

Mothersill C and Seymour C. 2006. Radiation-induced bystander effects: evidence for an adaptive response to low dose exposures? Dose-Response 4:283-290

Nagasawa H, Huo L and Little J. 2003. Increased bystander mutagenic effect in DNA double-strand break repair-deficient mammalian cells. Int J Radiat Biol 79:35-41

Nikjoo H and Khvostumov I. 2003. Biophysical model of the radiation-induced bystander effect. Int J, Rad Biol 79:43-52

Pant MC, Liao X-Y, Lu Q, Molloi S, Elmore E and Redpath JL. 2003. Mechanisms of suppression of neoplastic transformation in vitro by low doses of low LET radiation. Carcinogenesis 24:1961-1965

Persaud R, Zhou H, Baker SE, Hei TK and Hall EJ. 2005. Assessment of Low Linear Energy Transfer Radiation-Induced Bystander Mutagenesis in a Three-Dimensional Culture Model. Cancer Res 65:9876-9882

Redpath JL. 2006. Suppression of neoplastic transformation in vitro by low doses of low LET radiation. Dose-Response 4:302-308

Redpath JL and Elmore E. 2007. Radiation-induced neoplastic transformation in vitro, hormesis and risk assessment. Dose-Response 5:123-130

Sachs R, Hahnfeld P and Brenner D. 1997. The link between low-LET dose-response relations and the underlying kinetics of damage production/repair/misrepair. Int J Radiat Biol 72:351-374

Semenenko V and Stewart R. 2004. A Fast Monte Carlo Algorithm to Simulate the Spectrum of DNA Damages Formed by Ionizing Radiation. Radiat Res 161:451-457

Semenenko V, Stewart R and Ackerman E. 2005. Monte Carlo Simulation of Base and Nucleotide Excision Repair of Clustered DNA Damage Sites. I. Model Properties and Predicted Trends. Radiat Res 164:180-193

Seymour C and Mothersill C. 2000. Relative Contribution of Bystander and Targeted Cell Killing to the Low-Dose Region of the Radiation Dose–Response Curve. Radiat Res 153:508-511

Snyder AR. 2004. Review of radiation-induced bystander effects. Hum Exp Toxicol 23:87-89

Sofou S. 2008. Radionuclide carriers for targeting of cancer. Int J Nanomedicine 3:181-199

Sokolov MV, Smilenov LB, Hall EJ, Panyutin IG, Bonner WM and Sedelnikova OA. 2005. Ionizing radiation induces DNA double-strand breaks in bystander primary human fibroblasts. Oncogene 24:7257-7265

Stewart R. 1999. On the complexity of the DNA damages created by endogenous process. Radiat Res 152:101-104

Stewart R. 2004. VC Simulator (Virtual Cell Radiobiology Simulator), Resources for information on VC simulator package. Available at http://rh.healthsciences.purdue.edu/

Stewart R, Ratnayake R and Jennings K. 2006. Microdosimetric Model for the Induction of Cell Killing through Medium-Borne Signals. Radiat Res 165:460-469

Tavares A and Tavares J. 2010a. ^{99m}Tc Auger Electrons for Targeted Tumour Therapy: A Review. Int J Radiat Biol 86:261-270

Tavares A and Tavares J. 2010b. Evaluating ^{99m}Tc Auger Electrons for Targeted Tumor Radiotherapy by Computational Methods. Med Phys 37:3551-3559

UNSCEAR. 2007. Report of the United Nations Scientific Committee on the Effects of Atomic Radiation to the General Assembly, Vienna, Austria

Table 1. Input conditions for VC simulator.

Summary of VC Key Input Conditions	References
MODEL specification: DRM (damage repair model)=TLK CKM (cell kinetics model)=QECK (quasi-exponential cell kinetics model)	*(Stewart 2004)*
Cell parameters: DNA (cell DNA content)=5.667E+09 base pair NC (number of chromosomes per cell)=46 TPOT (cell doubling time)=0.667 or 1.625 days for fibroblasts and human crypt cells, respectively GF (growth fraction, if 0 (zero) all cells are quiescent, if 1 (one) all cells are cycling and if 0.5 the cell population is heterogeneous)=0.5 N0 (initial number of cells)=1000 KAP (peak cell density)=1.0E+38 cells/cm^3 VOL (tissue volume)=1 cm^3	*(Stewart 2004)* *(Stewart 2004)* *(Baserga 1971; Baserga 1993)* *N.A.* *N.A.* *(Stewart 2004)* *(Stewart 2004)*
Endogenous DNA damage parameters: DSB (endogenous)=4.3349E-03 Gy^{-1} $cell^{-1}$	*(Stewart 2004)*
Biophysical parameters: RHT (repair half-time)=XXX, XXX=0.25 9 h (simple DSBs are repaired faster than complex DSBs) ETA (pairwise damage interaction rate)=2.5E-04 h^{-1} PHI (probability of a misrejoined DSB being lethal)=0.005 A0 (probability of correct repair)=AAA, AAA=0.95 0.25 (simple DSBs are repaired more accurately than complex DSBs) GAM (fraction of binary-misrepaired damages that are lethal)=0.25 FRDL (fraction of residual that is lethal damage)=0.5	*(Stewart 2004)*
Key simulation stopping criterion: ACUT (absolute residual-damage cutoff)=1.0E-09 expected number of DNA damages per cell	*(Stewart 2004)*
Radiation exposure parameters: BGDR (average background absorbed dose rate on planet Earth)=2.73748E-07 Gy/h DCUT (dose cutoff used to truncate dose rate function after fraction 1-DCUT of total dose has been delivered)=0.01 Gy LAM (radioactive decay constant)=dependent on radionuclide used RHL (radionuclide half-life)=dependent on radionuclide used TCUT (time cutoff parameter)= 2 hours SAD (absorbed dose delivered in time interval 0-TCUT)=RX1, RX1=0.01 0.015 0.02 0.1 0.15 0.2 1 1.5 2 4 6 8 Gy STOL (step-size tolerance)=0.01 Gy/h	*(UNSCEAR 2007)* *(Stewart 2004)* *N.A.* *N.A.* *N.A.* *N.A.* *(Stewart 2004)*

N.A. = not applicable.

FIGURE CAPTIONS

Fig. 1. Number of human fibroblasts (a) and human crypt cells (b) that survived irradiation with distinct radioactive particles (low- and high-LET particles) and different absorbed doses. Note the parabolic type relationship between absorbed dose and estimated number of surviving cells. Modelled conditions: time of radiation exposure = 2 hours, initial number of cells = 1000 and simulator stopping criterion for cell count following radiation exposure: ACUT=1.0D-09 expected number of DNA damages per cell.

Fig. 2. Results from mutagenesis and enhanced genetic instability probability per surviving cell following exposure to different radiation sources and distinct absorbed doses. The probability per surviving cell following irradiation represents the probability of an altered gene function or expression causing enhanced genetic instability.

Fig. 3. Neoplastic transformation frequency per irradiated cell (a) and per surviving cell (b), expressed in $week^{-1}$, following exposure to different radiation sources and distinct absorbed doses.

Fig. 4. Average number of direct lethal damages per surviving cell after irradiation with distinct radioactive particles and different absorbed doses. Note the rapid increase in the number of lethal mutations per cell as a function of absorbed dose and different cellular dose-response curves depending on particle LET.

FIGURES

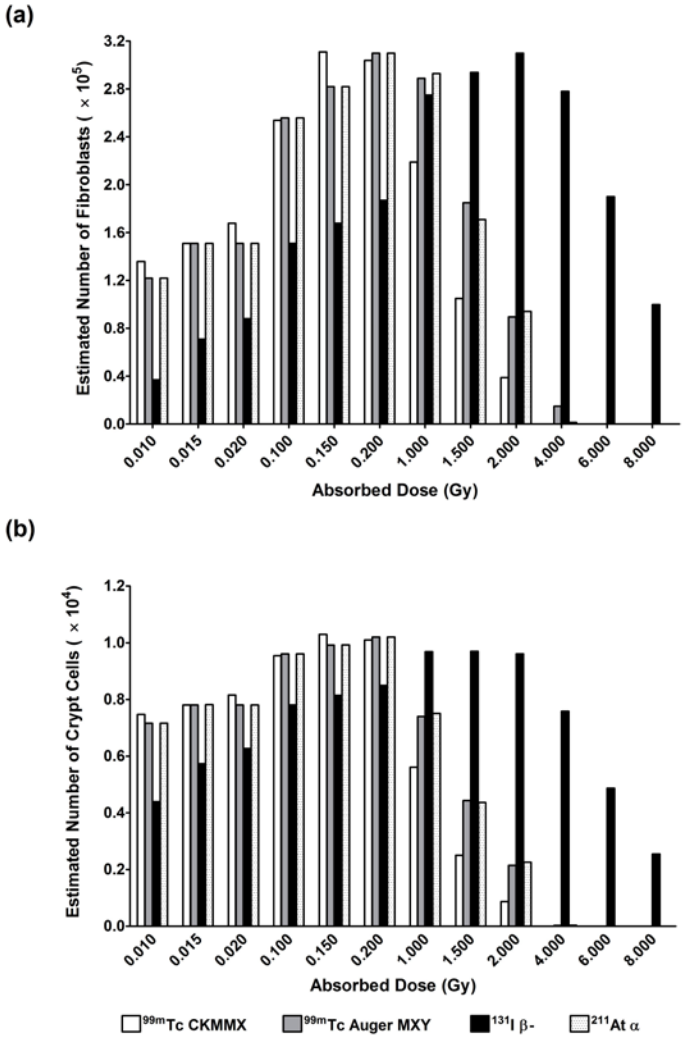

Figure 1

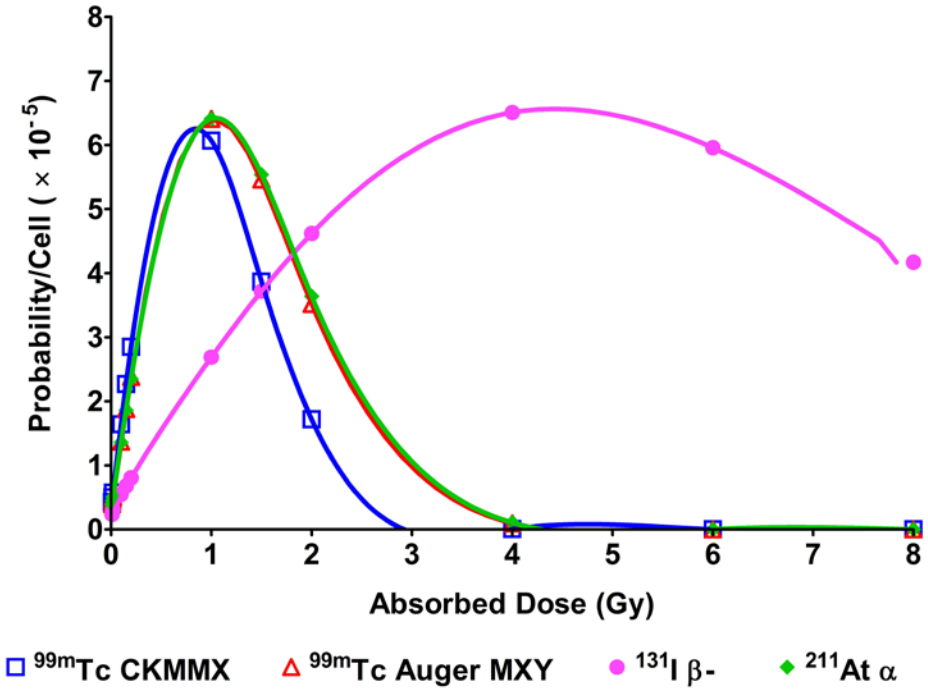
Probability/Cell (× 10-5)
Absorbed Dose (Gy)
99mTc CKMMX
99mTc Auger MXY
131I β-
211At α

Figure 2

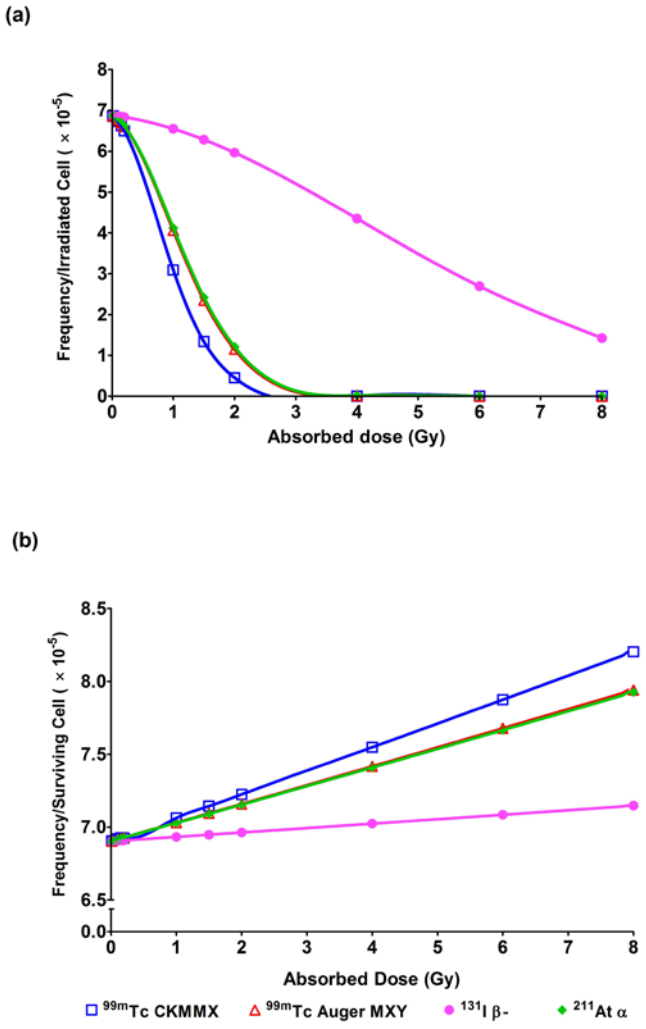
(a)
Frequency/Irradiated Cell (× 10^-5)
Absorbed dose (Gy)
(b)
Frequency/Surviving Cell (× 10^-5)
Absorbed Dose (Gy)
99mTc CKMMX
99mTc Auger MXY
131I β-
211At α

Figure 3

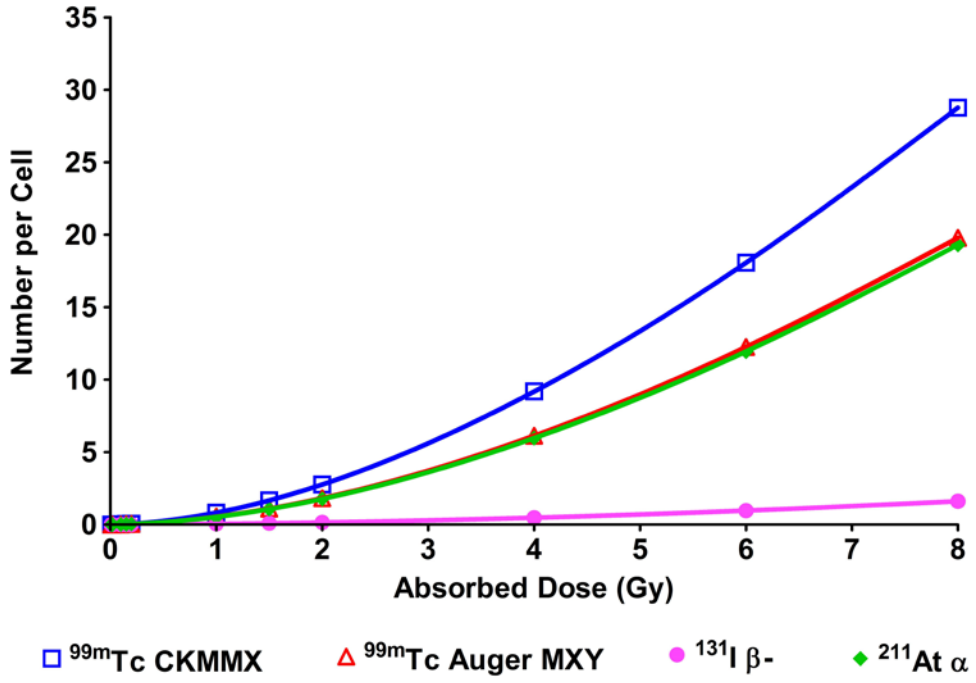
Number per Cell
35
30
25
20
15
10
5
0
0
1
2
3
4
5
6
7
8
Absorbed Dose (Gy)
99mTc CKMMX
99mTc Auger MXY
131I β-
211At α

Figure 4